Spokesman: V. E. Barnes
Physics Department
Purdue University
West Lafayette, Indiana 47906
317-749-2961

Fermilab Proposal No. 598

PROPOSAL FOR A HIGH-STATISTICS STUDY OF $\bar{P}P$ AND π^-P INTERACTIONS AT 50 GeV WITH THE FERMILAB 30-INCH HYDROGEN BUBBLE CHAMBER HYBRID SPECTROMETER WITH DOWNSTREAM PARTICLE IDENTIFIERS

Florida State University
Talahassee, Florida 32306

J. R. Albright
R. W. Diamond
S. L. Hagopian
V. Hagopian
J. Lannutti
W. Morris

Purdue University
West Lafayette, Indiana 47906

V. E. Barnes
D. D. Carmony
L. Dauwe
L. J. Gutay
C. N. Kennedy
L. K. Rangan
D. Zissa

C. R. N. Strasbourg
67037 Strasbourg, France

H. Braun
A. Fridman
J. P. Gerber
T. Juillot
N. Kurtz
G. Maurer
A. Michalon
C. Voltolini

January 1978

ABSTRACT

We propose to study with high statistics the interactions of 50 GeV antiprotons and negative pions in hydrogen, with charged forward particle identification and with tagging of forward antineutrons. Particular emphasis will be placed on the antiproton annihilation process, which will be identified by efficient tagging of the non-annihilation events. The annihilating system will be compared with the non-annihilating system, with the $\pi^- p$ system, and with the pp system, utilizing the full multiparticle detail of the bubble chamber together with the information on identities of forward particles. The energy is chosen to favor both inclusive particle production studies and the study of exclusive channels which, together with annihilation, decrease in cross section with increasing energy. Resonance production, and its relation to inclusive particle production, clusters and correlations, and its relation to the differences between annihilations and other hadronic processes, can also be studied in detail at this energy and with the advantages of particle identification. The center of mass energy of the annihilating system is in the range of energies of the hadronic system produced in Fermilab antineutrino and neutrino experiments. The two hadronic systems show striking similarities and merit a detailed comparison. Particle identification will permit tests of quark collision models dealing with particles produced at low transverse momenta.

REQUEST

1×10^6 pictures with established 50 GeV "halo" enriched $\bar{p}/\pi^-$ beam.

1×10^5 pictures with 50 GeV proton beam.

I. Summary of Proposed Experiment

We request 1×10^6 pictures of $\bar{p}p$ and $\pi^- p$ interactions in the Fermilab 30-inch bubble chamber hybrid spectrometer with the new Downstream Particle Identifiers (ISIS and a large segmented Cherenkov counter), and with the existing tagged negative beam (35% $\bar{p}$, 65% π^-). This study is a high statistics extension of the recent 50 GeV $\bar{p}p$ experiment, E-344, with the added facility of identifying a substantial number of outgoing charged particles in the forward center of mass hemisphere. In addition we wish to use the neutral hadron calorimeter to identify events with a leading $\bar{n}$, which in conjunction with the DPIs will permit the efficient identification of most of the non-annihilation events and provide an enriched sample of $\bar{p}p$ annihilations. We expect 140,000 $\bar{p}p$ interactions in the proposed exposure, of which 18,000 will be annihilation events.

We also expect 140,000 $\pi^- p$ events in this exposure. We propose to include in the first pass measurement of $\bar{p}p$ events those $\pi^- p$ events for which the DPIs indicate a potential non-pion tag for one or more tracks.

We also request a supplemental exposure of 100,000 pictures of pp interactions for physics comparisons at 50 GeV and to calibrate precisely the efficiencies of the downstream devices including the hybrid spectrometer, the DPIs and the neutral hadron calorimeter. We expect 35,000 pp interactions in this exposure.

II. Physics Interests of Proposed Experiment

A major purpose of the experiment is to study in detail many properties of the $\bar{p}p$ annihilating system at $\sqrt{s}$ = 9.7 GeV, and to compare with the non-annihilation events, the pp events, and the π^-p events at the same value of $\sqrt{s}$. There will be approximately 18,000 annihilation events as estimated by $\sigma_{ann} \approx \sigma_{tot}(\bar{p}p) - \sigma_{tot}(pp) = 5.7$ mb. In both the annihilation and the non-annihilation systems and in the π^-p events we can study multi-particle correlations, local conservation of quantum numbers, clusters, resonances, and the relations between them in new detail with forward charged particle identification. Neutral strange particles will be observed in significant numbers and can be correlated with charged kaons (see Figure 1) and with pions. Partial cross sections and event counts for the $\bar{p}p$ and π^-p interactions are shown in Tables I and II. Some kinematically fitted exclusive channels are relatively copious in the non-annihilation events, and can not only be studied in detail but can also be eliminated as possible annihilation events. Such channels can also be studied in the π^-p interactions. Inclusive single particle distributions can be studied in the tagged annihilation sample as well as in the non-annihilation, π^-p and pp events, and illuminating comparisons can be made.

Quark collision models now exist which describe particle production at low transverse momenta, in the fragmentation region and possibly into the more central part of the CM system (Das and Hwa[1], Duke and Taylor[2]). With particle identification we can study this region in detail in the non-annihilation events and the π^-p events, and may gain further insights into the nature of the contrasting annihilation process. The application of these models to π^-p interactions with identified particles in the beam fragmentation region is interesting because of the valence antiquark in the beam. Data on

charged particle ratios as discussed by Duke and Taylor now exist only for the proton target hemisphere. The $\pi^- p$ particle ratios will probe the sea quarks, and, given a valence antiquark distribution $x\bar{u}(x)$ concentrated at small x (Feynman and Field[3]), the sea distribution will be probed at values of x smaller than for pp collisions.

The hadronic system produced in lepton-lepton and lepton-hadron collisions resembles the system formed in $\bar{p}p$ annihilations, and none of these systems resembles the hadronic system arising from projectile fragmentation as seen in pp collisions and in non-annihilation $\bar{p}p$ collisions[4] (see Figures 2 and 3). At $\sqrt{s} = 9.7$ we can extend knowledge of the hadronic system in $\bar{p}p$ annihilation to cover more fully the range of W found in Fermilab antineutrino and neutrino experiments. The question of whether f_2^{--} continues to decrease linearly with $\langle n_c \rangle$ for $\bar{p}p$ annihilations is open, and a high statistics determination of this moment with a tagged sample of annihilations will shed light on the degree of similarity of the various hadronic systems at higher values of $\sqrt{s}$.

The measured $\bar{p}p$ annihilation cross section below 12 GeV fits reasonably well with the $\bar{p}p$ - pp total cross section difference measured at higher energies, with an overall $p_{LAB}^{-0.61}$ dependence (Figure 4). To date, the high energy multiplicity distribution in annihilations has been estimated by subtraction of the $\bar{p}p$ and pp inelastic topological cross sections, σ_n, which would imply that it is the inelastic cross section difference (also plotted in Figure 4) which relates to the annihilation cross section. A well-tagged annihilation sample should help in answering questions such as this.

While 50 GeV is already a high energy for the study of inclusive processes, it is still low enough that momentum resolution permits the study of some exclusive channels, which will also have larger cross sections than at higher energies. For inclusive resonance production studies, the somewhat lower

average charged particle multiplicity will tend to reduce the troublesome combinatorial backgrounds. One topic of particular interest is the possible baryonium meson states which prefer to decay into $N\bar{N}$ with or without extra pions, such as have been observed, for example, in CERN Omega spectrometer experiments [5,6] with cross sections as large as 1μb at 16 GeV/c. The inclusive baryonium production cross sections at 50 GeV are uncertain, but if any are substantially larger than 1μb we might be able to observe such states. In the $\pi^- p$ interactions such states would be tagged by a forward p or $\bar{p}$. In the $\bar{p}p$ interactions, where one might particularly expect the possibility of larger cross sections, the useful tag would be a forward proton.

Other resonances, which will be copious, include ρ^o, f^o, $K^*(890)^{+,-,o}$, φ, $\Delta^{++}(1238)$ and its antiparticle. Inclusive studies of the vector mesons will shed light on the fraction of pseudoscalar mesons which are the decay products of vector mesons, and on the ratio of K^* to ρ production, and on whether these ratios take on anomalous values in the case of annihilation. In the $\pi^- p$ events, observed K^o decays in addition to identified charged kaons will permit K^* production studies over the full pion beam hemisphere.

Another bonus of charged kaon identification is the possibility of testing the Okubo-Zweig-Iizuka (OZI) rule using a technique of Bloebel et al.[7]. By plotting all +− mass combinations as K^+K^- when one of the particles is known to be a kaon, the narrow φ signal will be cleanly observed. A search can then be made for extra $K^{+,-,o}$. Neither Bloebel et al.[7] at 24 GeV, nor Akerlof et al.[8] in a 400 GeV double arm spectrometer experiment on proton-nucleus collisions see evidence for an excess of kaons in conjunction with φ, in contradiction to the OZI rule.

III. Beam and Bubble Chamber

E-344 was run in the 30-inch hybrid bubble chamber in October, 1976, using the enriched $\bar{p}$ beam from antilambda decay. Measurement of $\bar{p}p$ events was completed in 1977. The overall beam composition as measured by the beam Cherenkov counter is $\bar{p}$ = 38%, π^- = 61%, and 1% ambiguous tag. This was achieved with a modest flash trigger enrichment, requiring at least two $\bar{p}$ into the bubble chamber per beam ping. Under these conditions we obtained 10^5 useful triads in one week of running. Given very good uniformity of beam flux from ping to ping the picture taking rate could have been even greater. A modest further gain in rate could be achieved by reducing the trigger requirement to ≥ 1 $\bar{p}$ per ping. We would expect to use the identical beam in the proposed experiment.

For the pp exposure we would simply reverse the beamline polarity and take protons from the lambda decay "halo". We have briefly tested this method at 60 GeV, where it gave a very large ratio of protons to π^+.

The existing system of upstream proportional wire chambers and either one of the beam Cherenkov counters will provide clean tagging of $\pi^{\pm}$, p and $\bar{p}$.

IV. Downstream Systems

The systems which we request to use are described in V. Kistiakowsky's article in NALREP, p. 13 (July 1976) and in proposals P-570 and P-394. The configuration which we shall discuss below is shown in Figure 5 . There are four essential parts: (a) forward proportional wire chambers and drift chambers for improved momentum resolution on fast forward particles, (b) ISIS, a 1m x 1m x 3m long device which uses many samples of the relativistic rise of ionization in a gas to identify charged particles with laboratory momenta between ~5 GeV/c and ~40 GeV/c, (c) an eight-cell atmospheric pressure Cherenkov counter of dimensions 2 x 2 x 5m^3, and (d) a neutral hadron calorimeter of transverse dimensions 31" x 31", to detect antineutrons. One important use of ISIS and the Cherenkov counter is to identify forward antiprotons. This capability in conjunction with the antineutron detector and with the capability of identifying slow protons by ionization in the bubble chamber, permits highly efficient identification of the non-annihilation channels having a nucleon and an antinucleon in the final state.

(a) The momentum resolution of the hybrid system of PWC's and drift chambers is $\Delta p/p=0.06p\%$ where p is in GeV/c. Thus particle momenta will be rather well determined at 50 GeV. And this momentum resolution will be more than adequate for the functioning of ISIS.

(b) While kaon identification becomes poor above about 40 GeV in the ISIS, pions traversing the ISIS are correctly identified over 98% of the time and (anti) protons are correctly identified 85% of the time from 50 GeV/c down to the low momentum cutoff which sets in rapidly between 10 and 5 GeV/c (see Figure 6). This matches well the geometrical acceptance of the downstream devices, which begins in the 5-10 GeV/c region (see section (e) below).

(c) With a proton threshold set just above 50 GeV/c, the Cherenkov

counter will correctly identify nearly all antiprotons which strike the 1.4m x 1.4 segmented mirror. At 100 GeV, 3.6% of the $\bar{p}$'s will have at least one other charged particle in the same mirror and thus fail to register as $\bar{p}$. At 50 GeV, the average charged particle multiplicity and forward charged particle density per unit solid angle are both smaller, and we estimate the above inefficiency to become less than 1.8%. This lower track density will be helpful to avoid confusions in all parts of the DPI, including the ISIS in particular. The Cherenkov counter in conjunction with the ISIS will provide highly efficient identification of non-annihilation events having a forward $\bar{p}$.

The Cherenkov counter also complements the ISIS by separating π/K between 7.5 and 27 GeV/c, separating π/p between 7.5 and 51 GeV/c, and K/p between 27 and 51 GeV/c. Kaons below their 27 GeV/c threshold, which might register in the Cherenkov counter as antiprotons and be lost from the annihilation sample, will tend to be identified by the ISIS.

(d) The neutral hadron calorimeter proposed in P-394 is a steel-scintillator sandwich neutron counter, of cross section 31" x 31" located 12m downstream from the center of the bubble chamber. This device is estimated to tag 80% of the $\bar{n}$ from 100 GeV interactions. We conservatively estimate that this figure is $\geq$ 69% for 50 GeV interactions, by scaling the $\bar{n}$ laboratory angles and momenta up and down by the ratio of the incident beam momenta. This has a small overall effect on the efficiency for detecting the non-annihilation events which go into the final states $N\bar{N}X$, as will be discussed in section (f).

(e) Geometrical Acceptances Based on Measured 50 GeV/c $\bar{p}p$ Events

Tracks from our measured 50 GeV $\bar{p}p$ events, with laboratory momentum above 5 GeV/c were swum through the magnetic field of the bubble chamber and

tested for entering the useful apertures of systems (a) through (d) above. In Figure 7 we show the distribution in rapidity, y, for all negative tracks in the sample, for tracks (A) entering the upstream end of ISIS (and hence having some hybrid momentum determination), for tracks (B) traversing the full length of the ISIS, and for tracks (C) striking one of the eight Cherenkov mirror segments. In Figure 8 we show the same set of distributions for all positive tracks in the sample. The acceptances of the ISIS and the Cherenkov counter start in the forward part of the central region and become large in the beam fragmentation region. In terms of the Feynman x variable, the acceptances start at $x = 0$, become moderate in the region $x \sim 0.1$ to 0.2, and are large beyond $x \sim 0.3$. Of especial note is the nearly 100% acceptance of fast forward negative tracks, which include the $\bar{p}$'s in non-annihilation events.

Table III shows the fractions of positive and negative tracks which enter the downstream system, traverse the ISIS, and traverse the Cherenkov counter. Since particle discrimination in the ISIS begins in the 5 to 10 GeV/c region, and since the pion Cherenkov threshold will be at about 7.5 GeV/c, we note that 80% of negative tracks and 59% of positive tracks above 5 GeV/c will traverse the ISIS. Many of these tracks will also traverse the Cherenkov counter, to receive a double tag.

(f) Purity of the Annihilation Sample

Based on identification of slow protons in the bubble chamber, identification of antiprotons by the Cherenkov counter, and identification of antineutrons in the neutral hadron calorimeter, Whitmore (P-394) estimates at 100 GeV that 97% of all non-annihilation events will be identified as $\bar{p}pX$, $\bar{p}nX$, $\bar{n}pX$, or $\bar{n}\bar{n}X$. We estimate conservatively that this efficiency will be 93% at 50 GeV (see Table IV), while the annihilation cross section is

substantially greater. Given 5.7mb of annihilation, 8.2mb of fitted elastic scattering, and 1mb of fitted $\bar{p}p$ -- $\bar{p}p\pi^+\pi^-$, only 29mb of other non-annihilation events remain. Of this, 2.0mb will not be identified by the downstream systems, giving a sample containing all or most of the annihilations and 74% pure. It is possible that some of the remaining non-annihilation events can be isolated on the basis of their kinematic properties.

V. Measurements and Analysis

Our existing 50 GeV $\bar{p}p$ data from E-344 have all been measured on the Purdue SMP's, with on-line geometrical reconstruction. The pass rate is 98% and the momentum accuracy even on fast forward tracks is quite good. With the downstream track coordinate information folded in, we find comparable resolutions in the rapidity distributions of forward $\bar{p}$ and backward p from our sample of the 4-constraint reaction $\bar{p}p \rightarrow \bar{p}p\pi^+\pi^-$ (Figure 9). The $p\pi^+$ and $\bar{p}\pi^-$ mass resolutions in this sample are also comparable (Figure 10), and show substantial production of $\Delta(1238)$. There is a striking absence of 4-constraint fits to the annihilation reaction $\bar{p}p \rightarrow \pi^+\pi^+\pi^-\pi^-$, as is expected from the trends of this cross section at lower energies. This is an indication of the quality of the track measurements and of the possibility of identifying certain exclusive channels through kinematics. Purdue plans to measure the proposed film using the same system, with the possible substitution of the Hydra computer programs for the current TVGP-SQUAW programs.

Florida State will measure the film on image plane digitizers which have a demonstrated accuracy of better than 5 microns rms on the film, and a high measuring rate.

Strasbourg plans to measure the film using high precision film plane digitizers with TV magnification of the film image to decrease the setting errors. Strasbourg has contributed to the development of the Hydra software, which offers improved reconstruction of high momentum tracks, among other advantages.

REFERENCES

1. K. P. Das and R. C. Hwa, Physics Letters 68B, 459 (1977).

2. D. W. Duke and F. E. Taylor, FERMILAB-Pub-77/95-THY (Oct. 1977).

3. R. D. Field and R. P. Feynman, Phys. Rev. D15, 2590 (1977).

4. Properties of the Hadronic System Resulting from $\bar{\nu}_\mu$ p Interactions, M. Derrick et al. (Argonne-Purdue-Carnegie Mellon) to be published in Phys. Rev.

5. Bari-Bonn-CERN-Daresbury-Glasgow-Liverpool-Milano-Purdue-Vienna Collaboration, C. Evangelista et al., Physics Letters 72B, 139 (1977).

6. P. Benkheiri et al., Physics Letters 68B, 483 (1977).

7. V. Bloebel et al., Physics Letters 59B, 88 (1975).

8. C. Akerlof et al., Phys. Rev. Letters 39, 861 (1977).

Table 1

$\bar{P}P$ Interactions in 1 x 10^6 Pictures

Beam: 35% $\bar{p}$; 3.2 events/μb

n_c	No. of Events	σ(mb)
2 (el.)	26,400	8.22 ± 0.19[1]
2 (inel.)	20,400	6.4[2]
4	32,600	10.2
6	28,400	8.9
8	19,600	6.1
10	8,400	2.6
12	3,200	1.0
14	740	0.23
16	160	0.05
18	26	0.008
Total	140,000	$43.86 \pm .11$[3]
Annihilation	18,200	$\sim 5.7 \approx \Delta\sigma_{tot}(\bar{p}p - pp)$[3]
$V^o + n_c$	11,000	
$2V^o + n_c$	1,600	
$\gamma \rightarrow e^+e^-$	6,800	2.1 (visible)
K^o_s	4,200	1.3 (visible)
Λ	1,600	0.5 (visible)
4-prong 4-c	1,600	1.0

(1) Fermilab Single Arm Spectrometer Group, Phys. Rev. Lett. 35, 1195 (1975)

(2) All inelastic topological cross sections and V^o cross sections are based on 10^5 measured pictures of 50 GeV $\bar{p}p$ interactions.

(3) Carrol et al., Phys. Rev. Lett. 38, 928 (1974)

Table II

π^-p Interactions in $1x10^6$ pictures

Beam: 65% π^- ; 5.9 events/μb

n_c	No. of Events	(mb)
2 (el.)	19,700	3.33[1]
2 (inel.)	20,500	3.5
4	36,200	6.1
6	32,500	5.5
8	19,600	3.3
10	9,200	1.56
12	1,900	0.33
14	1,000	0.17
Total	140,000	20.5
V^o+n_c	17,500	3.0
$\geq 2V^o+n_c$	2,700	o.5

(1) Elastic cross section: Fermilab Single Arm Spectrometer Group, Phys. Rev. Lett. 35, 1195 (1975)

All other cross sections are based on measured π^-p interactions in 50 GeV $\bar{p}p/\pi^-p$ pictures.

Table III

Geometrical acceptances of downstream detectors for measured negative and positive tracks from 50 GeV $\bar{p}p$ interactions.

	Number of Tracks (-)	Number of Tracks (+)	% of Forward Tracks (-)	% of Forward Tracks (+)	% of Tracks with $p_{LAB} \geq 5$ GeV/c (-)	% of Tracks with $p_{LAB} \geq 5$ GeV/c (+)
All	24,999	25,007				
Backward CM	9,148	15,106				
Forward CM	15,851	9,901				
$p_{LAB} \geq 5$ GeV/c	10,399	3,581				
≥ 5 GeV/c AND:						
Enter ISIS	10,144	3,397	64%	34%	98%	95%
Traverse ISIS	8,291	2,099	52%	21%	80%	59%
Exit Cherenkov	6,649	1,487	42%	15%	64%	42%

All tracks except identified slow protons are transformed using m_{π}. Kaons and protons are therefore plotted with greater than their true rapidity in Figures 7 and 8.

Table IV

Nonannihilation Event Tagging Efficiency

Inclusive Final State	Fraction of All Nonannihilation Events	Efficiency x Fraction
$\bar{p}pX$	0.49	(1 - .03x.30).49 = .486
$\bar{p}nX$	0.21	.97x.21 = .204
$\bar{n}pX$	0.21	(1 - .30x.41).21 = .184
$\bar{n}nX$	0.09	.59x.09 = .053
Total	1.0	.927

Assumes $\bar{p}/\bar{n} = 0.7/0.3 = p/n$ and factorization

$\mathcal{E}(\bar{p}) = 97\%$; $\mathcal{E}(p) = 70\%$ by ionization in B.C. ; $\mathcal{E}(\bar{n}) = 59\%$

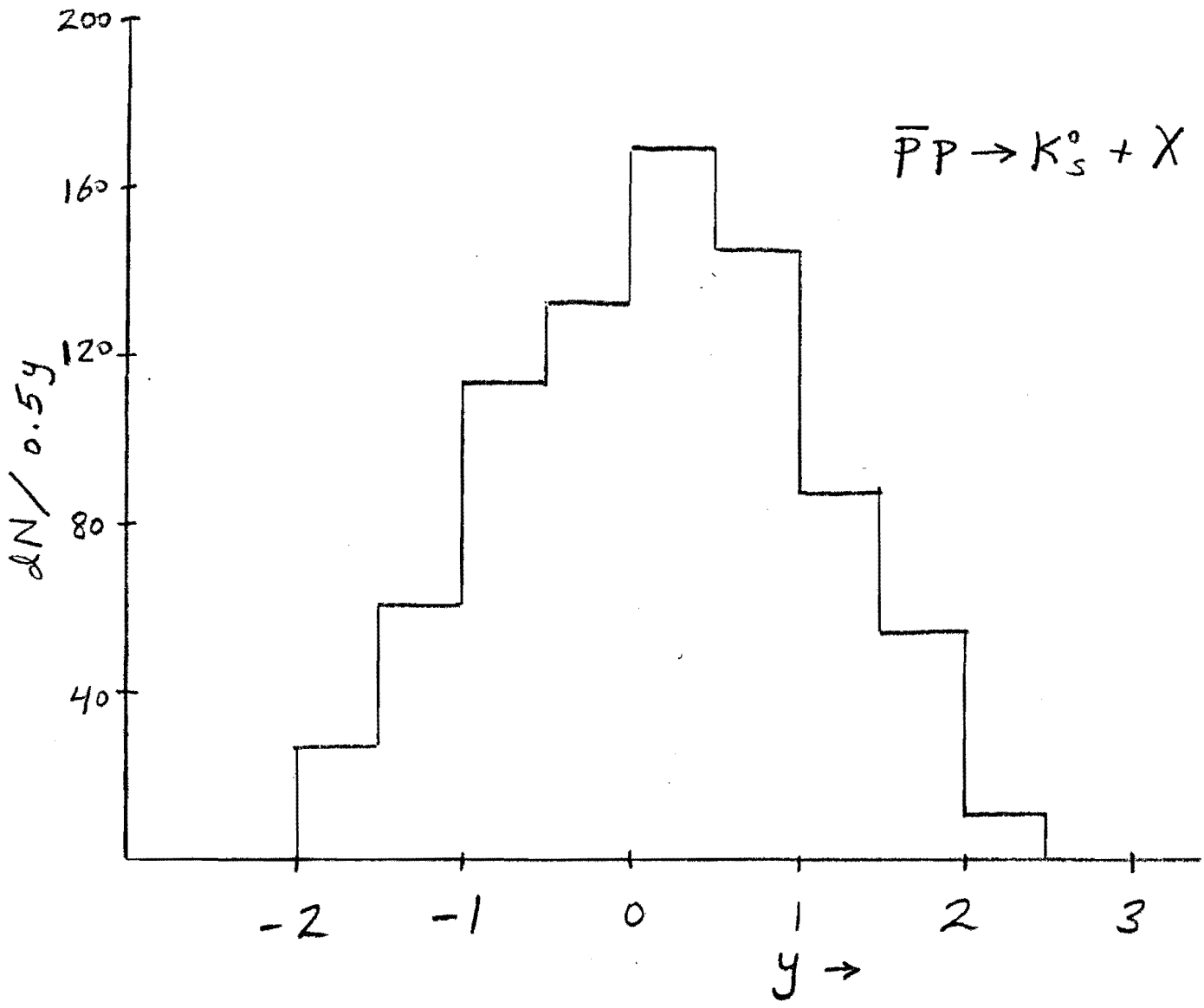

Figure 1. Rapidity distribution of K^0_S from 50 GeV $\bar{p}p$ inclusive interactions, weighted for ^0_S decay probability.

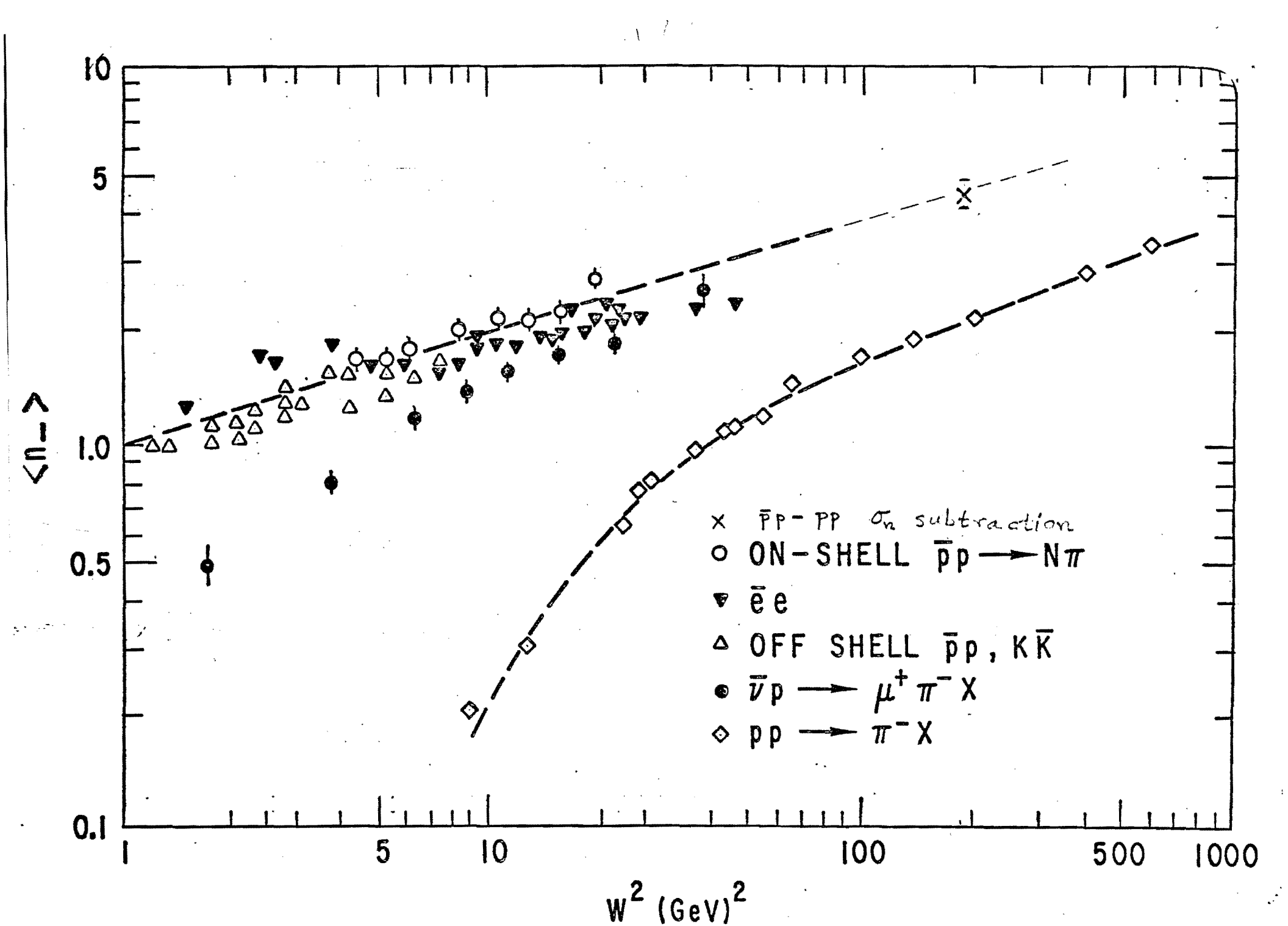

Figure 2. Average multiplicity of negative hadrons in various reactions, as a function of total hadronic mass squared. From Reference 4.

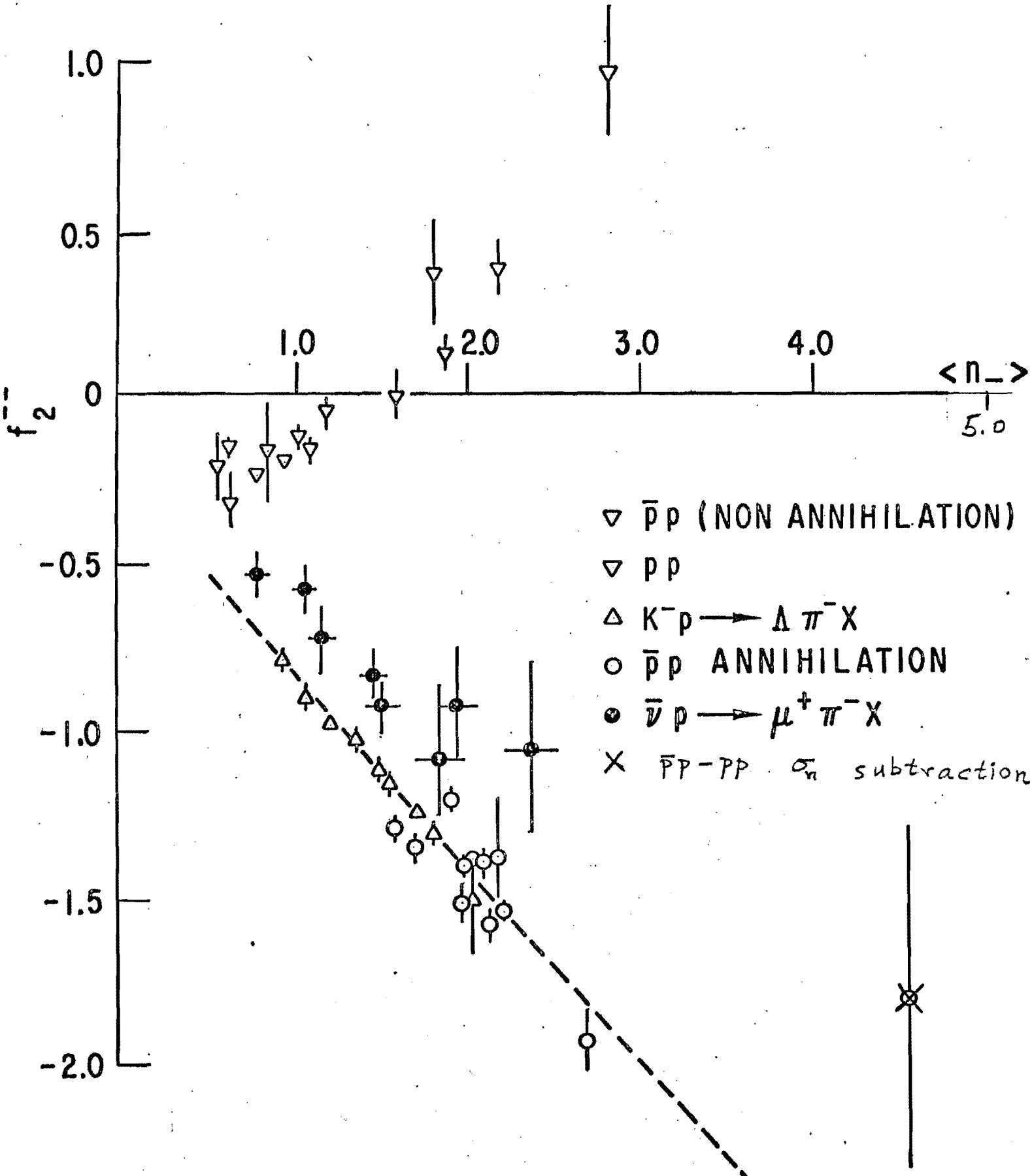

Figure 3. Two particle correlation moment f_2^{--} for various reactions as a function of mean negative hadron multiplicity. From Reference 4.

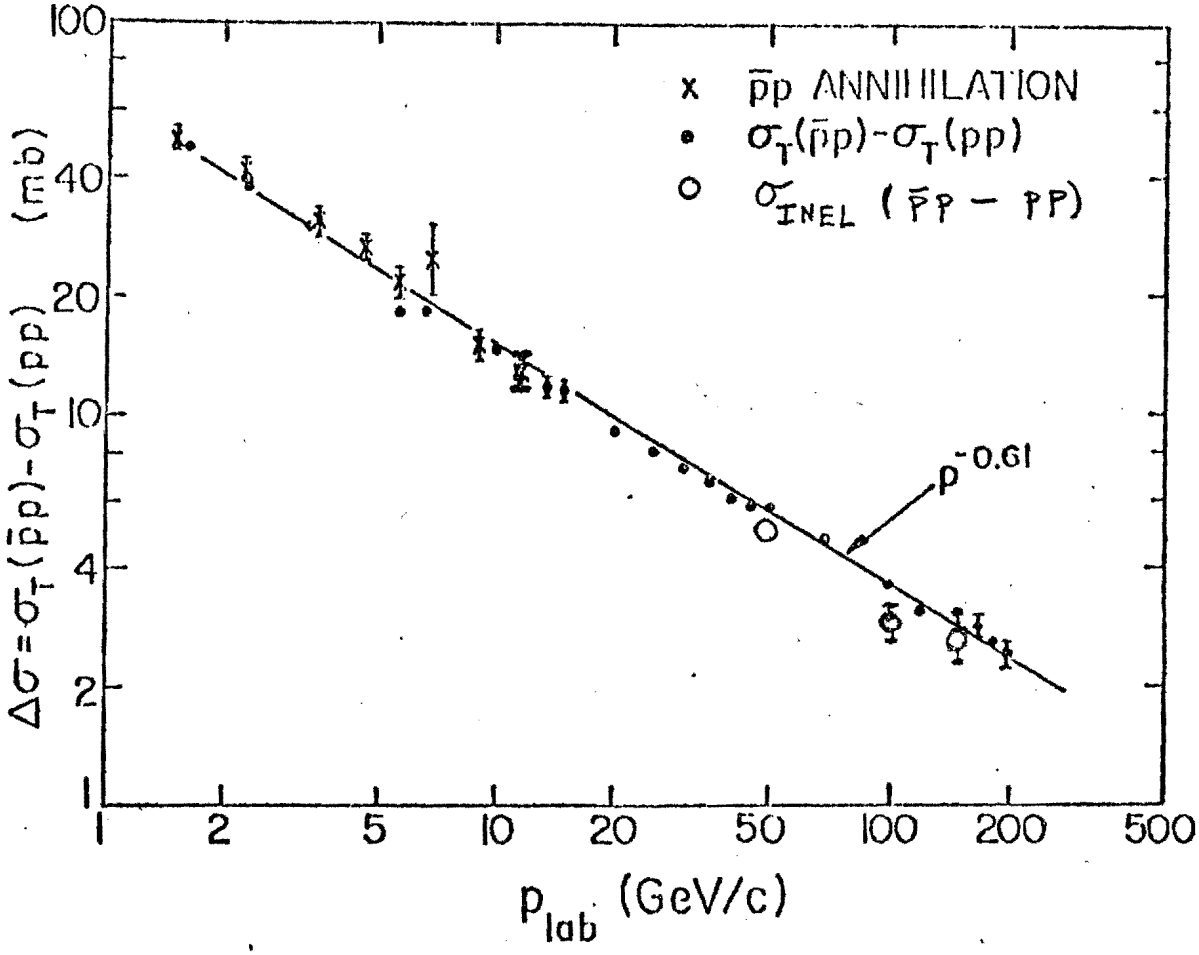

Difference in total cross section for $\bar{p}p$ and pp interactions as a function of the incident beam momentum. Also shown as the measured annihilation cross section at low energies (see J. Whitmore, proceedings of the APS/DPF Meeting, Seattle, 1975).

Figure 4. Points for difference in <u>inelastic</u> cross sections have been added.

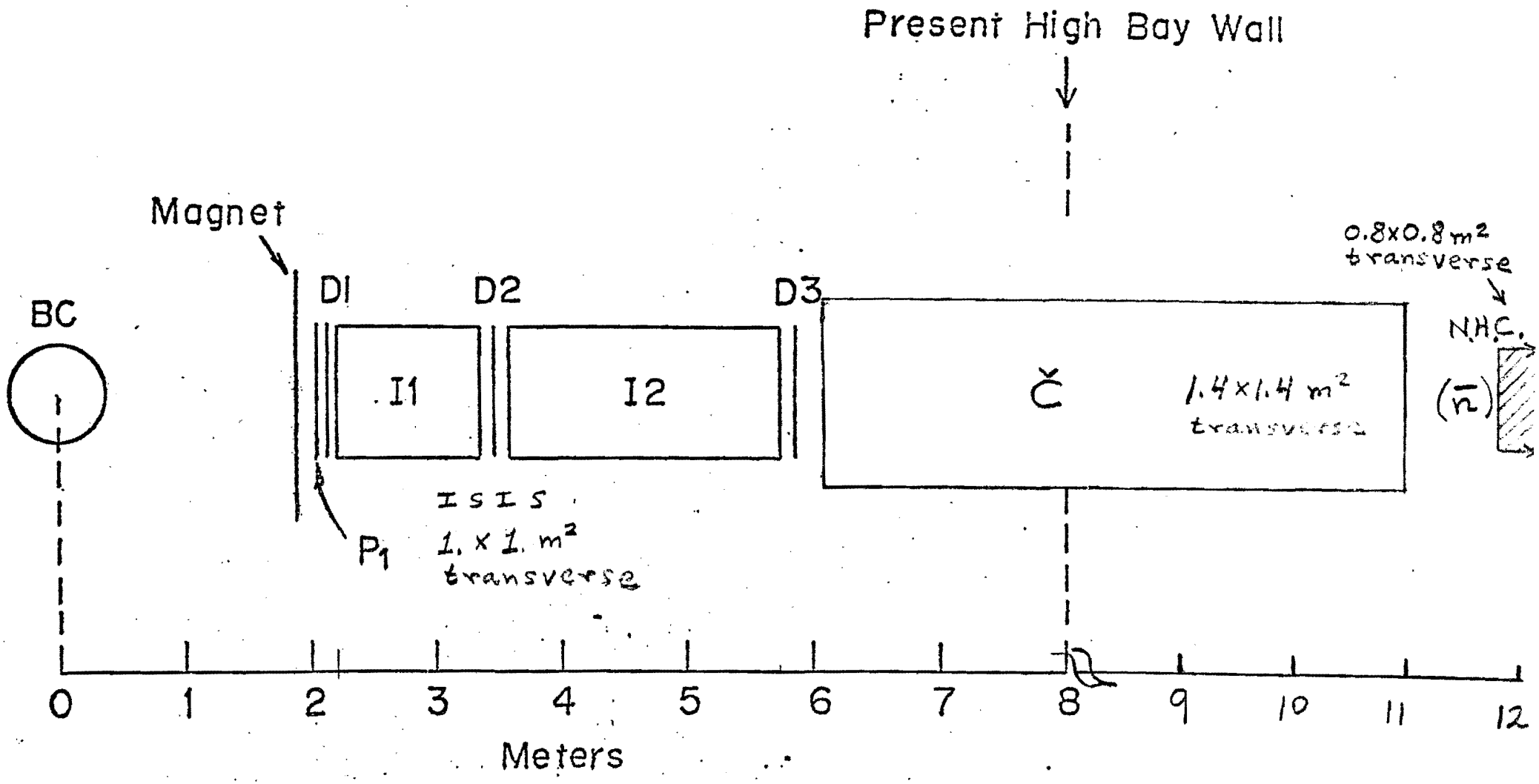

Figure 5. Proposed system of downstream position detecting and particle identifying devices, including Proportional Wire Chambers, P1; Drift chambers, D1-3; ISIS, I1 and I2; Cherenkov counter, Č; and Neutral Hadron Calorimeter, NHC ($\bar{n}$).

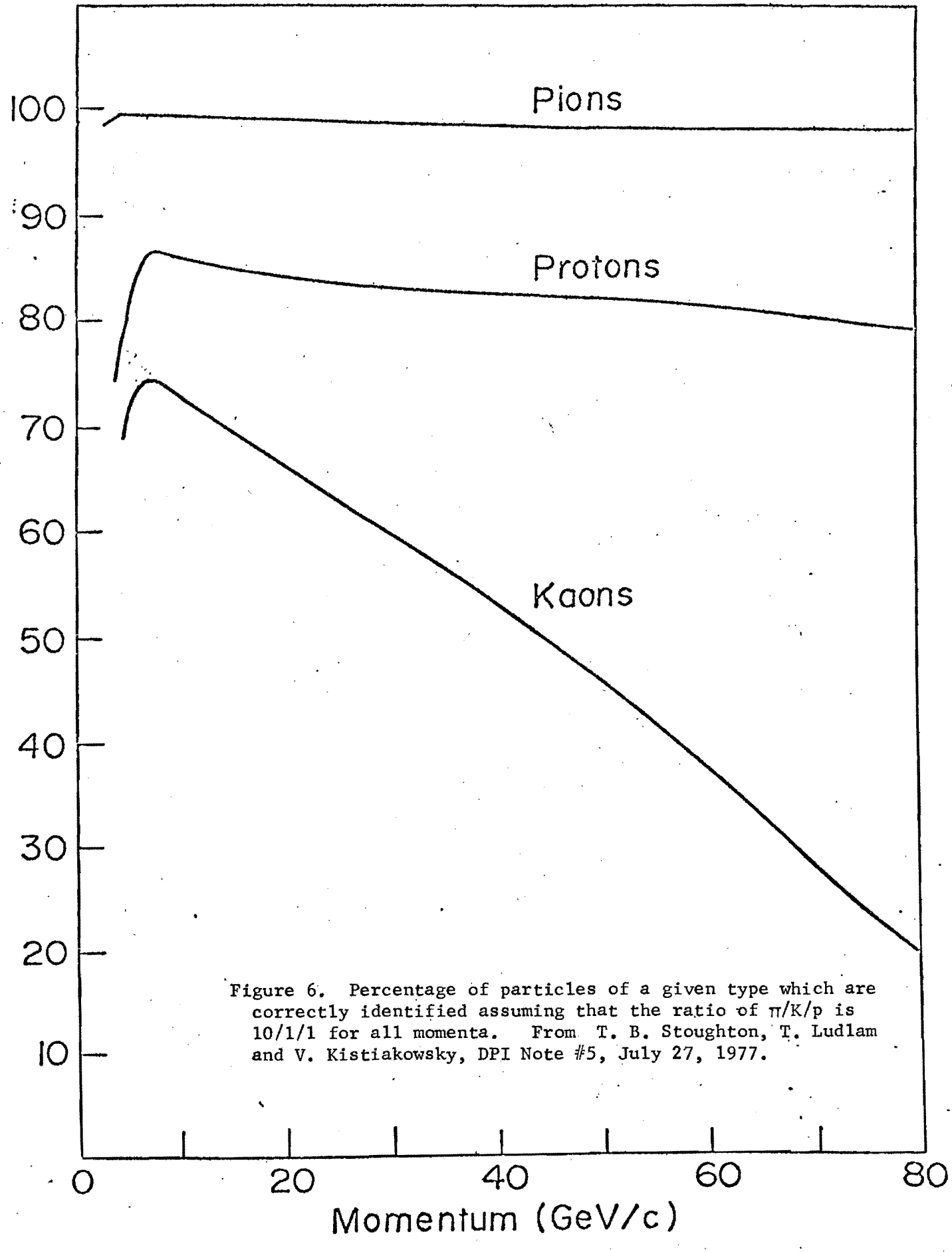

Figure 6. Percentage of particles of a given type which are correctly identified assuming that the ratio of $\pi/K/p$ is 10/1/1 for all momenta. From T. B. Stoughton, T. Ludlam and V. Kistiakowsky, DPI Note #5, July 27, 1977.

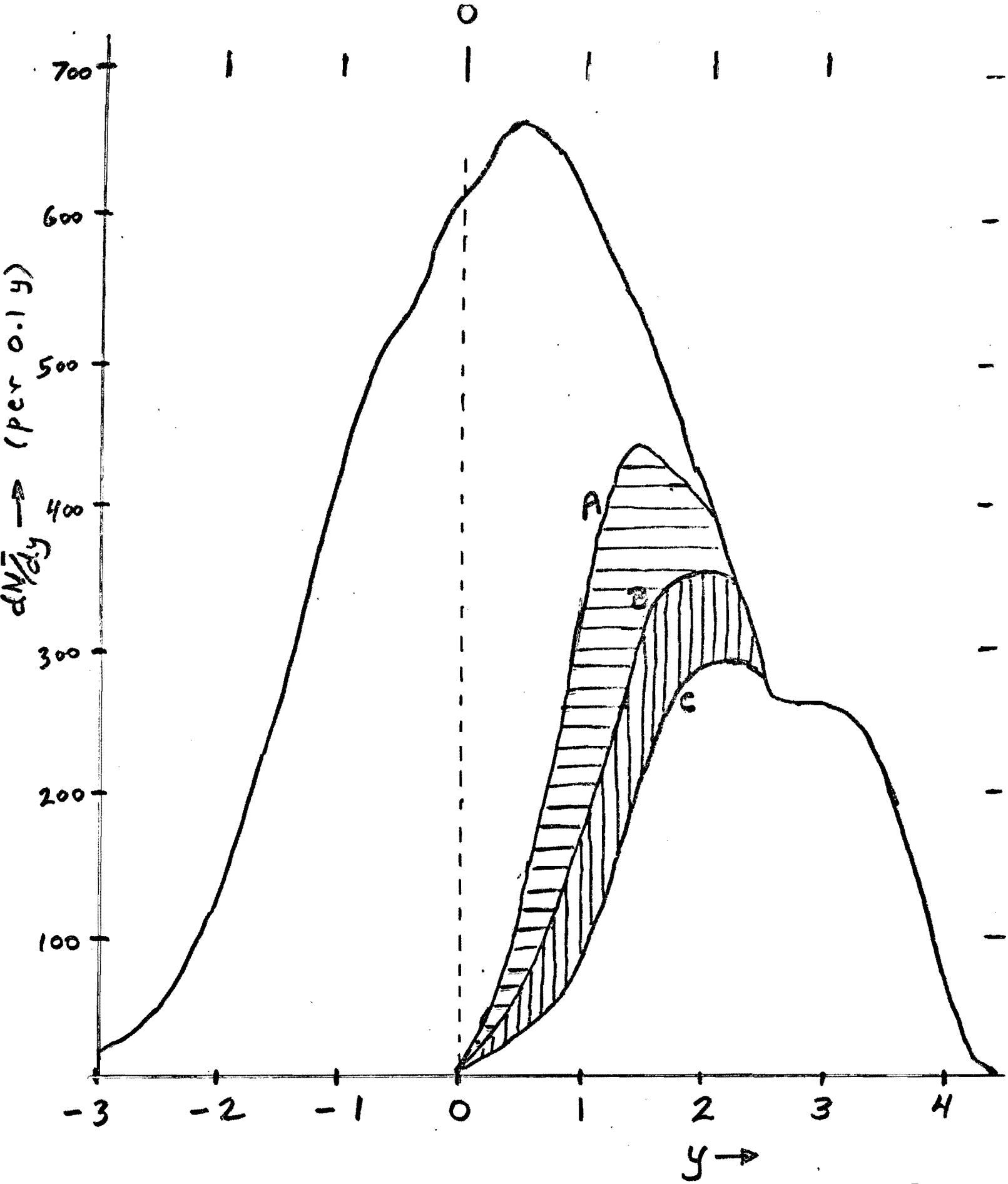

Figure 7. Rapidity distributions of all measured negative tracks from 50 GeV $\bar{p}p$ interactions, and for those tracks entering the useful apertures of (A) the first module of the downstream spectrometer; (B) traversing the full length of the ISIS; and (C) entering the mirror of the Cherenkov counte

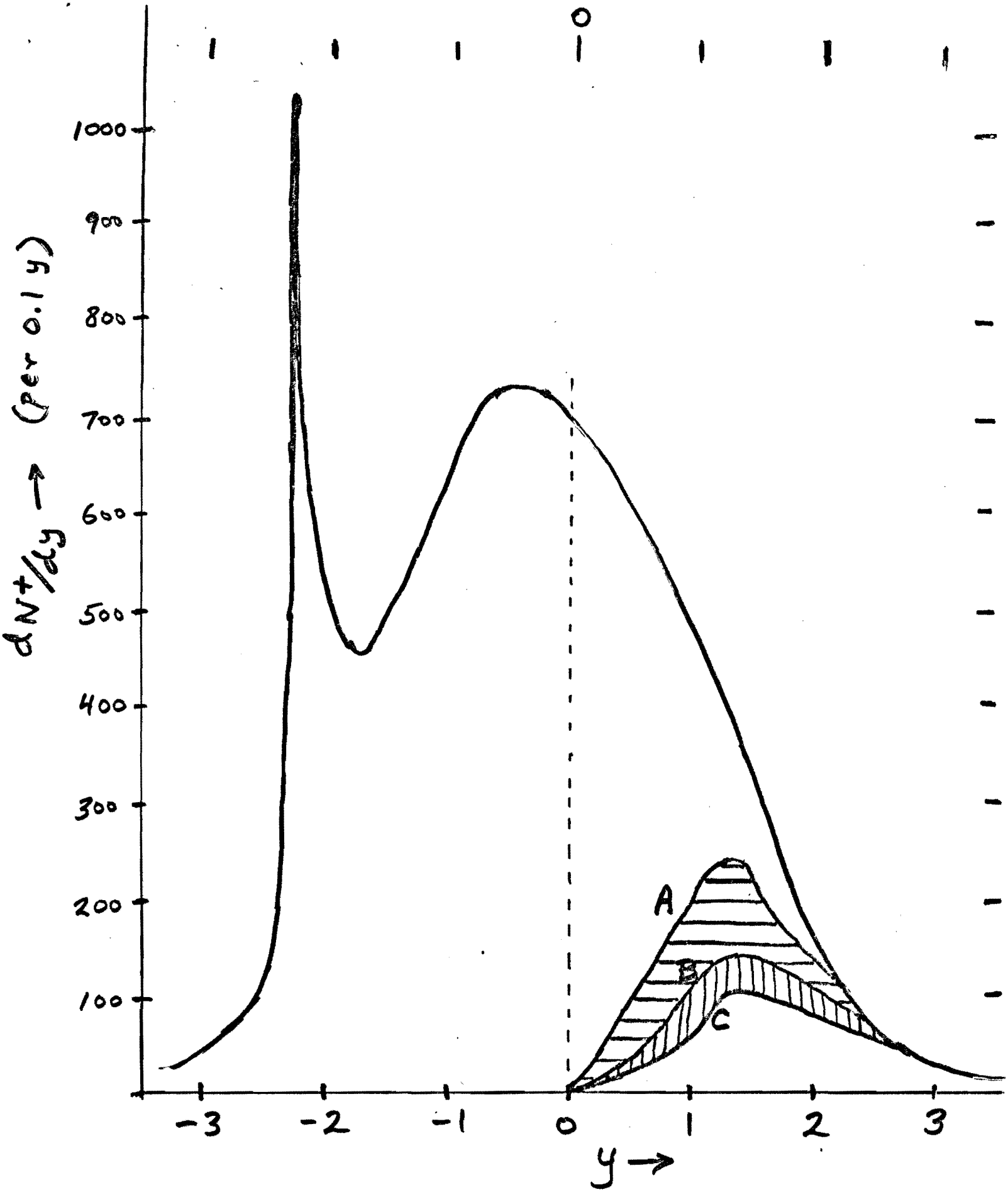

Figure 8. Rapidity distributions of all measured positive tracks, as described in Fig. 7.

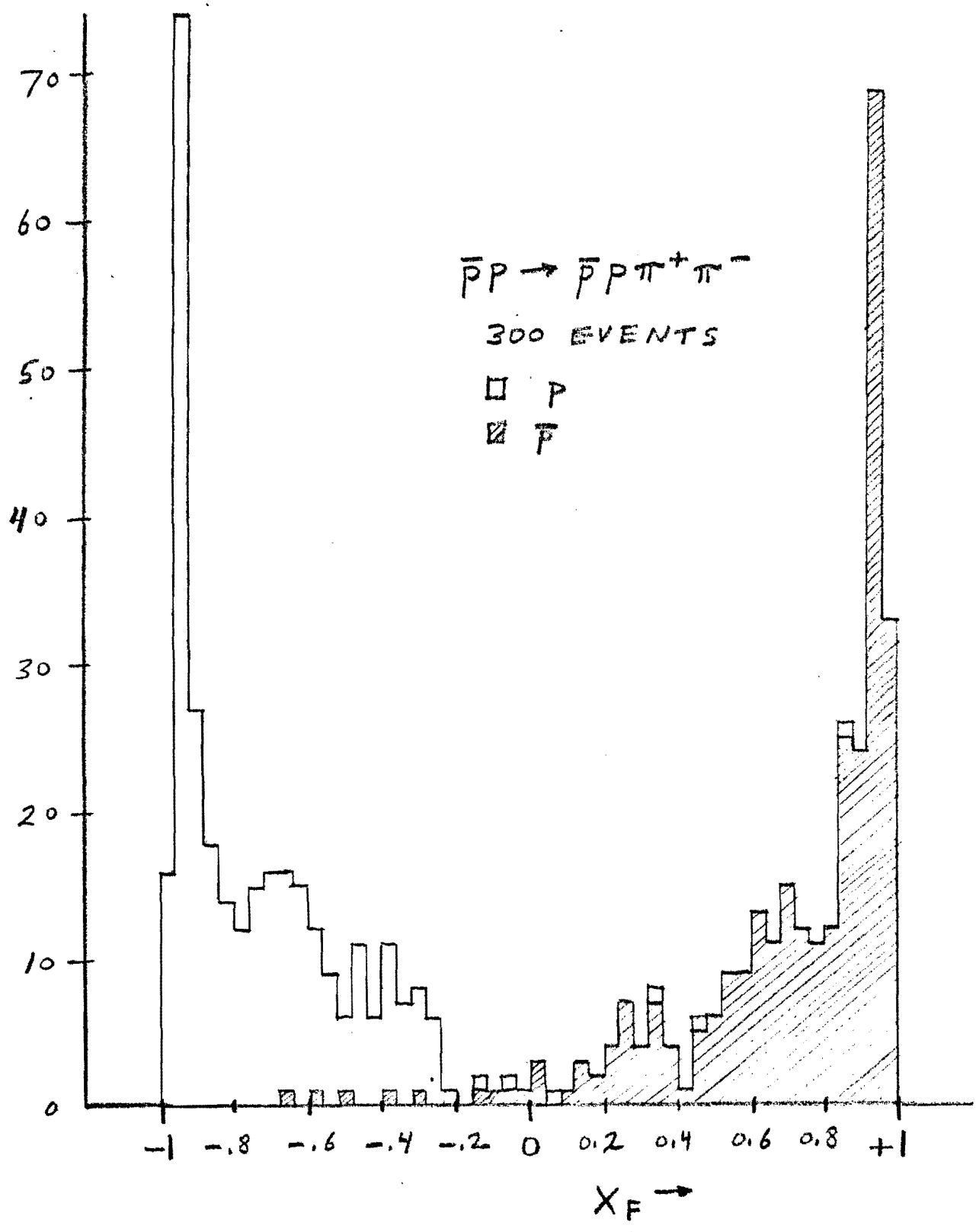

Figure 9. Feynman x distribution of protons and antiprotons from measured 4-constraint reaction $\bar{p}p \rightarrow \bar{p}p\pi^+\pi^-$ at 50 GeV.

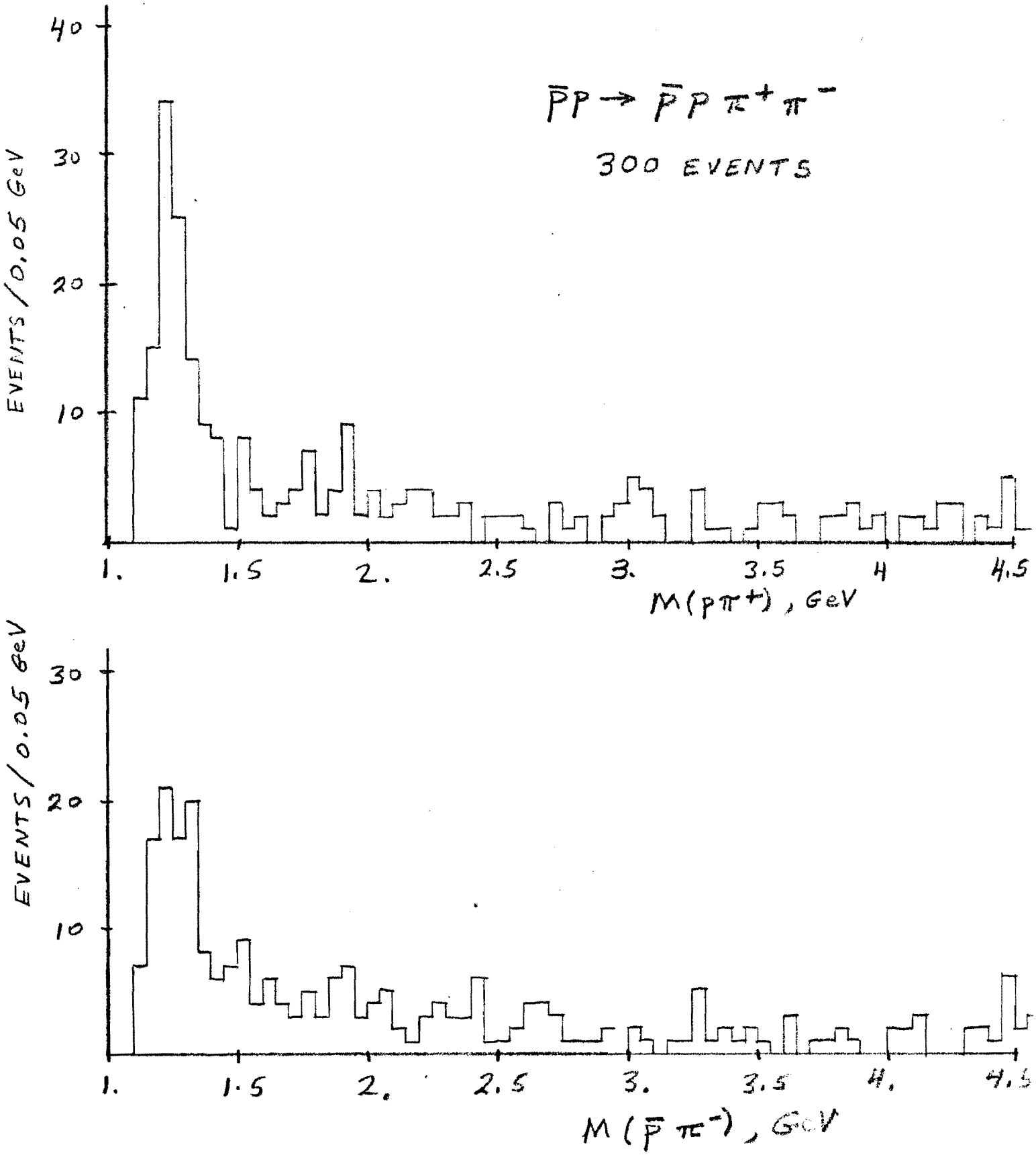

Figure 10. $p\,\pi^+$ and $\bar{p}\,\pi^-$ mass distributions from measured 4-constraint reaction $\bar{p}p \rightarrow \bar{p}p\pi^+\pi^-$ at 50 GeV.